

## Photoinduced chain fragment ordering in $\text{GdBa}_2\text{Cu}_3\text{O}_x$ thin films

S. O. Valenzuela

Facultad de Ciencias Exactas y Naturales, Universidad Nacional de Buenos Aires  
1428 Buenos Aires, Argentina

A. Faintein, P. Etchegoin, B. Maiorov, E. Osquiguil<sup>†</sup> and J. Guimpel<sup>†</sup>

Comisión Nacional de Energía Atómica, Centro Atómico Bariloche and Instituto Balseiro,\*  
8400 Bariloche, Río Negro, Argentina

We present Raman scattering experiments on oxygen deficient  $\text{GdBa}_2\text{Cu}_3\text{O}_x$  thin films as a function of illumination and annealing induced oxygen disorder. Raman lines due to copper and oxygen vibrations at the end of Cu-O chains are used to monitor the existence of chain fragments, and the dynamics of chain conjunction and fragmentation. The results indicate the presence of photoassisted oxygen ordering in the material.

PACS: 75.76.Bz, 78.30.-j, 73.50.Pz, 73.50.Gr

### 1. Introduction

The properties of the non-stoichiometric  $\text{RBa}_2\text{Cu}_3\text{O}_x$  family of high- $T_c$  compounds are known to depend strongly on the oxygen content  $x$  [1]. This is due to its layered perovskite structure, in which the Cu(1)O chains act as a charge reservoir for the Cu(2)O<sub>2</sub> planes, and also to the fact that the most labile ions are those of the chains. In this manner, changing  $x$  modifies the hole carrier concentration in the Cu(2)O<sub>2</sub> planes. It has also been found that for  $x < 7$  the configurational order of the remaining chain fragments determines the amount of transferred charge to the conduction planes [2].

Another interesting way to dope these compounds is through illumination. In oxygen deficient materials it has been shown that illumination with visible [3,4] or UV light [5] induces persistent photoconductivity (PPC) [3] and photoinduced superconductivity (PISC) [4]. In these phenomena an increase in the electrical conductivity,  $\sigma$ , and the superconducting critical temperature,  $T_c$ , are induced, which are persistent at temperatures below 250 K and relax through thermally activated processes at higher temperatures [6]. Although it is clear that the effect is due to trapping of photoinduced electrons and pumping of photoexcited holes to the conduction band, [3] the origin of the trapping mechanism remains controversial. Several scenarios have been proposed like photoassisted oxygen ordering [7] and trapping at oxygen vacancies [5].

The use of Raman scattering to study ordering of chain fragments has been hampered by the fact that Cu(1) and O chain ions occupy inversion centers and thus do not participate in Raman allowed modes. Oxygen order phenomena have been monitored in a rather indirect way by analyzing the line shape of the Raman allowed band due to the neighbor apical-oxygen vibrations [8,9]. Recent micro-Raman experiments of isotope substitution during local laser annealing by Ivanov *et al* [10] constitute a breakthrough to this situation: by observing the change of the mode frequency after a site selective  $^{18}\text{O} \leftrightarrow ^{16}\text{O}$

substitution, they were able to unambiguously assign two Raman bands located around  $248 \text{ cm}^{-1}$  and  $596 \text{ cm}^{-1}$  to vibrations of copper and oxygen atoms, respectively, at the end of short chain fragments. These modes, which are forbidden for infinite (or very long) chains, become Raman active due to loss of inversion symmetry of the atomic sites on chain fragmentation. The assignment of these "defect" modes is consistent with an earlier suggestion of Wake *et al* [11]. Subsequent detailed work by Iliev *et al* [12] has exploited these and other features of the Raman spectra to probe the transformation of the local oxygen arrangements (microdomains) with changes of oxygen content upon laser annealing.

### 2. Experimental details

We have used [13] these spectral lines to follow the evolution of the chain fragment distribution during annealing above room temperature at constant  $x$ , and during illumination with laser light, providing evidence for the conjunction of short chain fragments into longer chains under illumination. In order to test contrasting interpretations of the observed photobleaching in  $\text{YBa}_2\text{Cu}_3\text{O}_x$  [14], we have extended our Raman measurements to samples with other oxygen contents and complement it with absorption spectra of  $\text{GdBa}_2\text{Cu}_3\text{O}_x$  thin films.

The (001) textured oxygen deficient  $\text{GdBa}_2\text{Cu}_3\text{O}_x$  thin films were grown on (001) MgO and SrTiO<sub>3</sub> substrates by DC magnetron sputtering as described in reference 6. Prior to any Raman measurements the samples were annealed at room temperature (292 K) for several days. Raman spectra were collected with a triple Jobin-Yvon T64000 spectrometer provided with a liquid N<sub>2</sub>-cooled CCD camera. The 514.5 nm line of an Ar-ion laser was used for excitation in a backscattering geometry with parallel incident and scattered polarization ( $z(x,x)z$  configuration in Porto's notation). Laser powers ranging from 1 to 50 mW were focussed to a circular spot of  $\approx 100 \mu\text{m}$  diameter.

<sup>†</sup>: Also at CONICET, Argentina

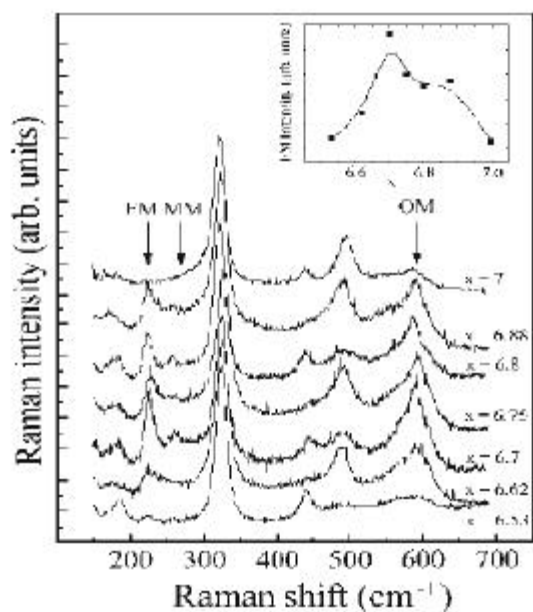


Figure 1: Room temperature Raman spectra of  $\text{GdBa}_2\text{Cu}_3\text{O}_x$  films for different  $x$ . The arrows indicate the position of the "forbidden" chain end oxygen, OM, and Cu, MM and FM, modes (see text for an explanation of the labeling) The inset shows the normalized intensity of the FM peak as a function of  $x$ .

During the illumination periods the light source for the photoexcitation was the same laser line used for Raman data collection. We verified that no significant laser induced heating of the sample was generated, by measuring Stokes and anti-Stokes components of the Raman spectra. In all cases the sample temperature and laser power density were such that changes of oxygen content due to in or out-diffusion [12,15] could be ruled-out. For the absorption experiments a halogen lamp was used as light source. The transmitted light was dispersed with the Raman spectrometer and detected by a photomultiplier with conventional photon counting techniques. The scanning times and light intensity were adjusted to prevent photoexcitation. Typical resolutions were  $2\text{-}3\text{ cm}^{-1}$  for the Raman scattering and  $2\text{ nm}$  for the absorption spectra.

### 3. Results and discussions

Figure 1 shows the room temperature spectra for films of different oxygen content. The known phonon lines due to Raman-active  $z$ -polarized modes are observed at  $160\text{ cm}^{-1}$  ( $\text{Cu(2)O}_2$  plane copper in-phase mode),  $330\text{ cm}^{-1}$  ( $\text{Cu(2)O}_2$  plane oxygen out-of-phase mode),  $435\text{ cm}^{-1}$  ( $\text{Cu(2)O}_2$  plane oxygen in-phase mode), and  $500\text{ cm}^{-1}$  (apical oxygen mode). Besides these modes, the two Raman "forbidden" bands due to chain fragment end vibrations at around  $248\text{ cm}^{-1}$  (Cu vibration) and  $596\text{ cm}^{-1}$  (oxygen vibration) are clearly seen. Several features are to be remarked on the data. First, the intensity of these bands is maximum at around  $x=6.7$  and drops to zero both at  $x=6.5$  and  $x=7$ . This is to be expected since at this  $x$  values the

structure of the  $\text{Cu(1)O}$  chains should tend to ortho II and ortho I, respectively, both composed of complete chains [12], increasing the average length of the fragments and thus reducing the number of chain ends. In a simplified picture we also expect the number of chain ends to be maximum at  $x=6.75$ . Second, the band at  $248\text{ cm}^{-1}$  consists of two distinct peaks at around  $225$  and  $260\text{ cm}^{-1}$ . Within the assignment of these peaks to Cu vibrations at the end of chain fragments, we tentatively interpret these peaks as a Cu-O-Cu monomer mode (MM,  $260\text{ cm}^{-1}$ ) and a longer Cu-O-...-O-Cu fragment mode (FM,  $225\text{ cm}^{-1}$ ). The reason for this assignment is twofold: i) the Cu-Cu nearest neighbor relative displacement is larger for the MM than for the FM, augmenting thus the stretching force energy and Coulomb repulsion, shifting the MM mode to higher frequencies; ii) if a local tetragonal order is assumed around the monomers, and given that the chain bond lengths are reduced for the tetragonal material [16], an increase in the force constants is expected, again shifting the MM mode to higher frequencies. Last, the  $330\text{ cm}^{-1}$   $B_{1g}$  mode shows a clear Fano effect asymmetry [17], evidencing a coherent interaction between this phonon and the electronic background, which greatly reduces with  $x$ .

The effect of illumination and thermal annealing are shown in figure 2. Panel (a) shows the optical bleaching of the MM, FM and OM modes under illumination at  $80\text{ K}$  for a sample quenched from room temperature. Panel (b) shows a clear increase of the same modes as the temperature is slowly increased above room temperature. If we interpret the intensity of the modes as a counter for the number of chain fragment ends in the sample, it follows that temperature increases the number of fragments and illumination decreases them, i.e. illumination induces photoassisted oxygen ordering [7]. Figure 3 shows the time and temperature evolution of the integrated intensity of the

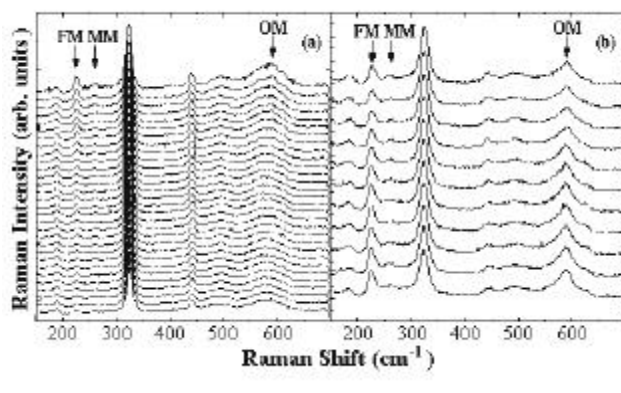


Figure 2: Raman spectra continuously taken with 10 minutes integration time for (a) illumination with  $50\text{ mW}$   $514.5\text{ nm}$  laser light at  $80\text{ K}$  after a rapid (5 min) quench from room temperature, (b) annealing with increasing temperature from  $295\text{ K}$  to  $375\text{ K}$ . Time and temperature increase from top to bottom. The spectra correspond to the sample with oxygen content  $x=6.8$ . The arrows indicate the position of the "forbidden" chain end oxygen, OM, and Cu, MM and FM, modes (see text for an explanation of the labeling)

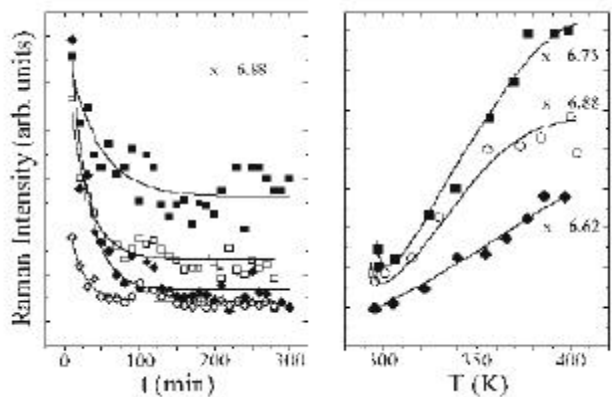


Figure 3: Intensity of the Raman lines, normalized to the intensity of the 330 cm<sup>-1</sup> line. Left panel, FM, squares, and MM, diamonds, intensity as a function of illumination time after a quench from room temperature, open symbols, and 400K, solid symbols (30mW 514.5 nm laser light at 80K). Right panel, FM intensity as a function of temperature for different oxygen contents. Lines drawn as are guides to the eye.

MM and FM modes, normalized to the 330 cm<sup>-1</sup> B<sub>1g</sub> mode, for different x and initial states. The bleaching of the MM is almost complete, independently of the history of the sample. However the final bleached state of the FM mode keeps memory of the initial disorder state of the sample. This result is consistent with that of reference 6, where it was found that the thermally induced disorder and the photoinduced order are not equivalent and do not cancel each other.

For oxygen contents lower than 6.88 the Cu(2)O<sub>2</sub> plane oxygen out-of-phase mode at 330 cm<sup>-1</sup> has a Lorentzian shape which does not depend on illumination. However, for x≥6.88 an asymmetry is developed that changes under illumination. This line was adjusted to a standard Fano function

$$I(\omega) = A \frac{(q + e)^2}{1 + e^2}$$

where A is a constant,  $e = (\omega - \omega_0) / \Gamma$ ,  $\omega$  is the Raman shift,  $\omega_0$  is the phonon frequency,  $\Gamma$  is the limiting Lorentzian linewidth, and q is the Fano asymmetry parameter. Figure 4 shows the evolution of  $\omega_0$  and q under illumination at 80K. The Lorentzian peak position for the x=6.62 sample is included for comparison. It is evident that the peak position and asymmetry parameter are affected by illumination, decreasing the asymmetry and shifting the line to higher  $\omega$ . The interpretation of this result is not straightforward since the trend seems to be opposite to that of figure 1. We believe it may indicate the reduction of density of states due to the opening of the photoinduced superconducting gap, since for x≥6.88 the data was acquired near T<sub>c</sub>. A detailed study of the Fano effect would imply modeling of the evolution of density of states and Raman matrix elements under illumination and will be the subject of a future publication.

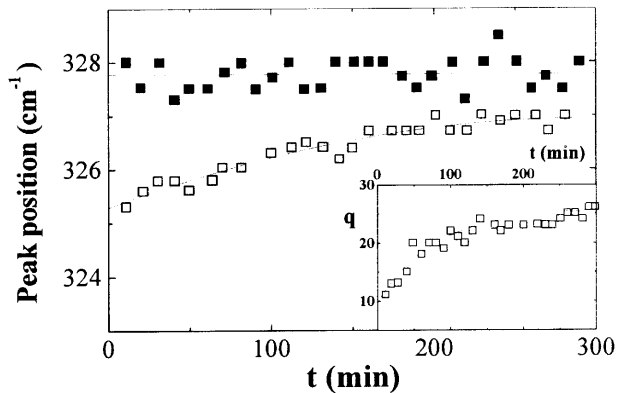


Figure 4: Line position for the 330 cm<sup>-1</sup> B<sub>1g</sub> mode as a function of illumination time for an x=6.62 sample with Lorentzian lineshape, solid squares, and an x=6.88 sample with asymmetric Fano lineshape, open squares. Inset shows the evolution of the Fano asymmetry parameter for the last sample. Lines are drawn as guides to the eye.

Recently, Käll et al interpreted the photoexcitation changes induced on Raman scattering in terms of photoinduced reduction of the number of "intermediate step resonant electronic states" [14], a contrasting scenario. In order to account for the x dependence of the intensity of the "forbidden" Raman lines, maximum around x=6.7 and zero for x=6.5 and x=7, they proposed that these electronic defect states should be localized at the chain ends. The most important fact supporting this model is the existence of a strong Raman resonance of the chain modes for laser

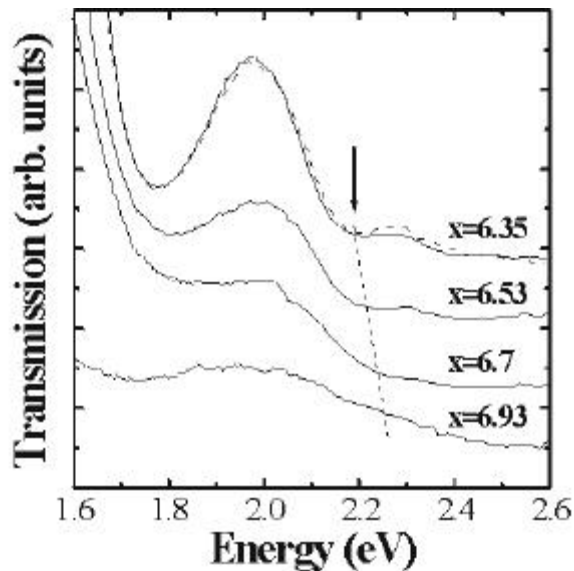


Figure 5: Transmission spectra at 77 K for films of different oxygen content. Note the small absorption around 2.2 eV, arrow and dashed line, probably associated with the "yellow resonance"[11] of the CuO-chain related additional modes. The dashed spectrum for x=6.35 was acquired without moving the sample after a long exposure to green laser light. No difference between the before and after illumination spectra was observed, within experimental error.

excitations around 2.2 eV [11], and the reported observation of a narrow absorption feature at that energy that, apparently, bleaches upon illumination [18].

In order to verify this point we performed low temperature, 80K, transmission measurements on films with oxygen content. In from  $x=6.35$  to  $x=7$ , before and after long exposures to high power green laser light, 514.5 nm. The films thickness of  $\sim 200$  nm was such that laser illumination along the full depth sensed by the transmission measurements could be assured. Representative data are displayed in Figure 5, for the energy region of interest. A small absorption is observed around 2.2 eV, that broadens and blue shifts with increasing  $x$ . This feature is clear for  $x=6.35$ , almost unobservable at  $x=6.7$ , and disappears in the "fully oxygenated" sample. These observations agree with the spectroscopic ellipsometry results reported by Kircher *et al* [19], and do not follow the same oxygen content dependence as the intensity of the "forbidden" CuO chain related Raman lines [13,14]. Moreover, we have not observed within our experimental error any difference between the spectra before and after laser light illumination. An example of this result is shown in figure 5 for  $x=6.35$ .

In conclusion, we have monitored the dynamics of Cu(1)O chain fragments in oxygen deficient  $GdBa_2Cu_3O_x$  films through Raman scattering intensity of lines assigned to chain end vibrations. Previous results [6] show that the order induced by illumination and thermal annealing are not equivalent. However, the results presented here clearly show that photoassisted oxygen ordering is present in the material.

We acknowledge J. Azcarate for help during sample preparation. Work partially supported by ANPCYT PICT97 03-00061-01117, CONICET PIP4207, Fundación Balseiro and Fundación Antorchas.

## References

\*: Dependent from Comision Nacional de Energía Atomica and Universidad Nacional de Cuyo.

- [1] See for example, L. H. Greene and B. G. Bagley, in *Physical Properties of High Temperature Superconductors II*, edited by Donald M. Ginsberg, 509 (World Scientific, Singapore, 1990).
- [2] B. W. Veal, A. P. Paulikas, H. Shi, Y. Fang, and J. W. Downey, *Phys. Rev. B* **42**, 6305 (1990); J. Kircher, E. Brücher, E. Schönherr, R. K. Kremer, and M. Cardona, *Phys. Rev. B* **46**, 588 (1992).
- [3] A.I. Kirilyuk, N.M. Kreines, and V.I. Kudinov, *Pis 'ma Zh. Eksp. Teor. Fiz.* **52**, 696 (1990) [*JETP Lett.* **52**, 49 (1990)].
- [4] G. Nieva, E. Osquiguil, J. Guimpel, M. Maenhoudt, B. Wuyts, Y. Bruynseraede, M. B. Maple and I. K. Schuller, *Appl. Phys. Lett.* **60**, 2159 (1992); G. Nieva, E. Osquiguil, J. Guimpel, M. Maenhoudt, B. Wuyts, Y. Bruynseraede, M. B. Maple and I. K. Schuller, *Phys. Rev. B* **46**, 14249 (1992).
- [5] T. Endo, A. Hoffmann, J. Santamaría and I. K. Schuller, *Phys. Rev. B* **54**, 3750 (1996).

- [6] J. Guimpel, B. Maiorov, E. Osquiguil, G. Nieva and F. Pardo, *Phys. Rev. B* **56**, 3552 (1997).
- [7] E. Osquiguil, M. Maenhoudt, B. Wuyts, Y. Bruynseraede, D. Lederman and I. K. Schuller, *Phys. Rev. B* **49**, 3675 (1994).
- [8] V. G. Hadjiev, C. Thomsen, J. Kircher, and M. Cardona, *Phys. Rev. B* **47**, 9148 (1993).
- [9] M. Iliev, C. Thomsen, V. Hadjiev, and M. Cardona, *Phys. Rev. B* **47**, 12341 (1993).
- [10] V. G. Ivanov, M. N. Iliev, and C. Thomsen, *Phys. Rev. B* **52**, 13652 (1995).
- [11] D. R. Wake, F. Slakey, M. V. Klein, J. P. Price, and D. M. Ginsberg, *Phys. Rev. Lett.* **67**, 3728 (1991).
- [12] M. N. Iliev, H. -U. Habermeier, M. Cardona, V. G. Hadjiev and R. Gajic, *Physica C* **279**, 63 (1997); M. N. Iliev, P. X. Zhang, H.-U. Habermeier and M. Cardona, *Journal of Alloys and Compounds* **251**, 99 (1997).
- [13] A. Fainstein, P. Etchegoin, and J. Guimpel, *Phys. Rev. B* **58**, 9433 (1998).
- [14] M. Käll, M. Osada, M. Kakihana, L. Börjesson, T. Frello, J. Madsen, N. H. Andersen, R. Liang, P. Dosanjh, and W. N. Hardy, *Phys. Rev. B* **57**, R14072 (1998).
- [15] V. G. Ivanov, M. N. Iliev and C. Thomsen, *Phys. Rev. B* **52**, 13652 (1995).
- [16] R. J. Cava, A. W. Hewat, E. A. Hewat, B. Batlogg, M. Marezio, K. M. Rabe, J. J. Krajewski, W. F. Peck Jr., and L. W. Rupp Jr., *Physica C* **165**, 419 (1990).
- [17] C. Thomsen, in *Light Scattering in Solids VI*, edited by M. Cardona, 326 (Springer, Heidelberg, 1983).
- [18] V. M. Dimitriev, V. V. Eremenko, V. G. Piryatinskaya, O. R. Prikhod'ko, and E. V. Khristenko, *Low. Temp. Phys.* **19**, 968 (1993).
- [19] J. Kircher, M. K. Kelly, S. Rashkeev, M. Alouani, D. Fuchs, and M. Cardona, *Phys. Rev. B* **44**, 217 (1991).